

PI-funnel control for two mass systems

Achim Ilchmann and Hans Schuster

May 25, 2007

submitted for publication to *IEEE Trans. on Automatic Control*

Abstract

We model a two mass system as a functional differential equation so that it encompasses friction and hysteretic effects. The structural properties, such as bounded zero dynamics, are investigated. We then propose three simple controllers (separately and in conjunction): a funnel controller, a PI-controller and a high-pass filter. As opposed to previous control strategies of two mass systems which invoke identification mechanisms or neural networks, the controllers in the present paper are based on structural properties of the system only. Despite the simplicity of the controllers, prespecified output behaviour with prespecified accuracy is guaranteed by the funnel controller, active damping of the shaft oscillation by the high-pass filter, zero tracking output error in the steady state by the PI-controller and bounded input disturbances are rejected. Finally, the controllers are implemented on a real plant, an electrical drive.

Index Terms

Adaptive control, tracking, two mass systems, electric drives.

1. INTRODUCTION

IN the present paper we model and control a nonlinear two mass system. The system is modelled as a single-input, single-output functional differential equation. Essentially, it is a three dimensional linear equation perturbed by a functional operator mainly modelling nonlinear friction, see (2.1) and Figure 1.2. The functional operator allows for hysteretic effects, dead zone effects and others.

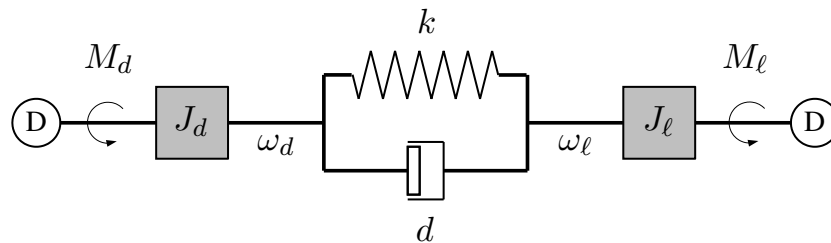


Fig. 1.1. Mechanical model of a two mass system.

In Figure 1.1, the mechanical model of the linear part of the two mass system is shown. Two electrical drives with mass moment of inertia J_d and J_l generate the torques M_d and M_l , respectively. The electrical machine D on the left hand side is considered as the drive, whereas the electrical machine D on the right hand side applies a load torque and emulates the mechanical system to be driven. The reaction of the mechanical system to the power train is substituted by an appropriate setting of the torque M_l . Hence, a wide variety of different

A. Ilchmann is with the Institute of Mathematics, Technical University Ilmenau, Weimarer Straße 25, 98693 Ilmenau, Germany. achim.ilchmann@tu-ilmenau.de

H. Schuster is with the Faculty of Electrical Engineering, Institute of Electrical Drive Systems, Technical University of Munich, Arcisstraße 21, 80333 Munich, Germany. hans.schuster@tum.de

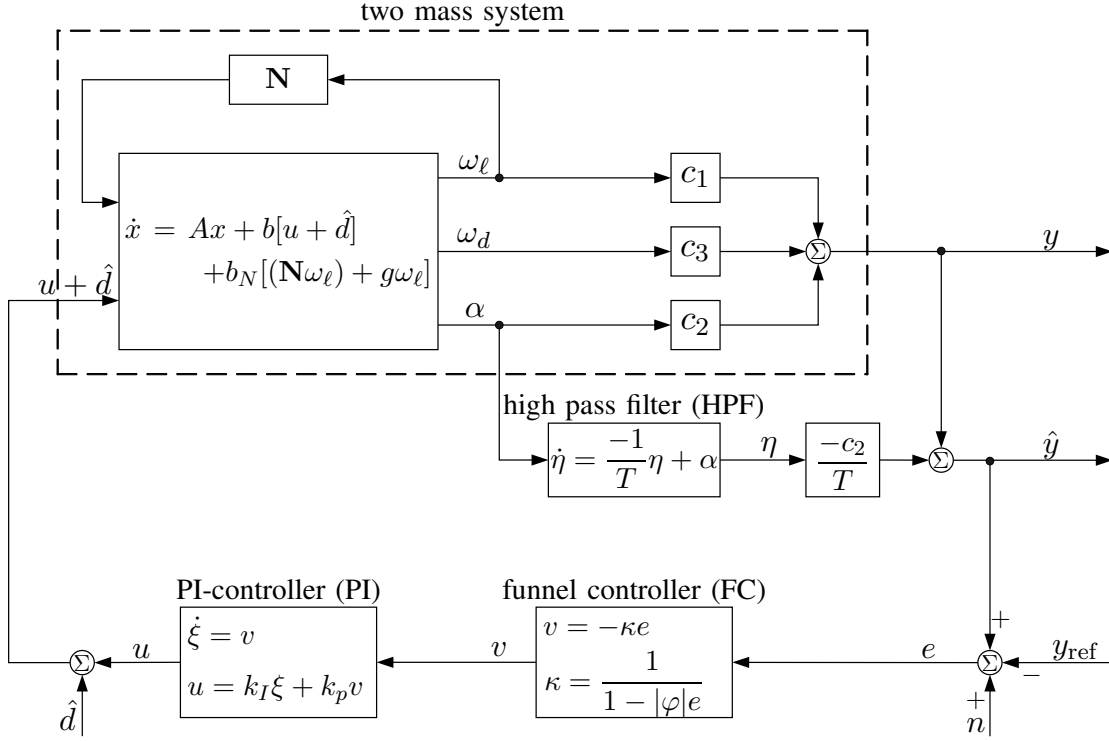


Fig. 1.2. Block diagram for the overall control loop.

mechanical systems is encompassed by this model. Moreover, the mechanics of the actual built plant (see experimental results in Section 6) remain fix while representing a large variety of different mechatronic systems. The behaviour of nearly all electric drives can be reproduced by this plant: for example the feed drive of a lathe in a tool machine or continuous processing plants such like rolling mills as well as flexible structures (for example robotic arms or read-write-heads of hard disc drives).

To transmit the torque, both electrical drives are connected by an elastic shaft. Although in most power trains the shaft is constructed as stiff as possible, some non-ideal behaviour remains always. This means that the shaft is elastic and acts like a spring damper system. For this reason, undesirable oscillations may occur and the speed ω_d does not necessarily coincide with ω_ℓ . The control objective is to inject a torque M_d such that the speed ω_ℓ converges to a desired reference signal, even if a load M_ℓ is applied.

In practical applications the parameters of the plant are usually unknown or uncertain. Over the last two decades, two mass systems have been adaptively controlled by identification mechanisms, neural networks or fuzzy methods [2]. Off-line identification of the plant parameters can only be applied to stable plants and it is difficult to decide when the identification is “good enough”. If online identification is applied, then closed-loop control and identification takes place simultaneously which may cause undesirable or unpredictable transient behaviour of the closed loop. Moreover, if the identification has to converge to the correct parameters, both strategies (off-line and online) suffer from the fact, that “persistence of excitation” is required for the input signals, see [8]. A widespread identification mechanism uses neural networks (NN), in particular radial base function network (RBF), general regression neural network (GRNN) and multi layer perceptron network (MLP) to approximate static nonlinearities of the system. If the parameters of the linear dynamics of the plant have to be identified (structured) recurrent neural networks (SRNN) are suitable [1]. However, minimizing the deviation between the output of the NN and the function itself is a non-convex optimization problem and results

in immense duration for the learning period, see [1].

In contrast to the above described control strategies, identification of the parameters is not required at all for the funnel controller (introduced by [4]) which is based on structural properties of the system only such as stable zero dynamics, relative degree one and known sign of the high-frequency gain. Moreover, the funnel controller has the appealing advantages that it obeys prespecified transient behaviour and guaranteed accuracy, tolerates measurement noise and nonlinear dynamic disturbances. However, the practical drawbacks of the funnel controller are that a non-zero steady state error usually remains and oscillations in the elastic shaft are not damped. Both drawbacks are overcome if the funnel controller is combined with a PI-controller and a high pass filter, see Figure 1.2. This had been suggested and investigated by Schuster et al. [9]. In the present paper we will extend this idea; moreover, we include input disturbances, a fairly large class of nonlinearity in the model and test all controllers on a real plant, which is an electric drive.

The paper is organized as follows. The model of a two mass system is introduced and its structural properties are analyzed in Section 2. In Section 3, we introduce the control objectives. Combinations of the three controllers (high-pass filter, PI-controller and funnel controller) are investigated in Section 4. Our main result on tracking is presented in Section 5. Experimental results of the control on a two mass system are shown in Section 6. Finally, the paper ends with some conclusions.

We close this introduction with remarks on notation. Throughout, $\mathbb{R}_{\geq 0} := [0, \infty)$ and \mathbb{C}_- denotes the open left half complex plane $\{\lambda \in \mathbb{C} \mid \operatorname{Re} \lambda < 0\}$. For an interval $I \subset \mathbb{R}$, $C(I \rightarrow \mathbb{R}^n)$ is the space of continuous functions $I \rightarrow \mathbb{R}^n$, $L^\infty(I \rightarrow \mathbb{R}^n)$ is the space of essentially bounded measurable functions $x: I \rightarrow \mathbb{R}^n$ with norm $\|x\|_\infty := \operatorname{ess-sup}_{t \in I} \|x(t)\|$, $L^\infty_{\text{loc}}(I \rightarrow \mathbb{R}^n)$ is the space of measurable, locally essentially bounded functions $I \rightarrow \mathbb{R}^n$, and $W^{1,\infty}(I \rightarrow \mathbb{R}^n)$ is the space of absolutely continuous functions $x: I \rightarrow \mathbb{R}^n$ with $x, \dot{x} \in L^\infty(I \rightarrow \mathbb{R}^n)$. The spectrum of $A \in \mathbb{R}^{n \times n}$ is denoted by $\operatorname{spec}(A)$.

2. THE MODEL

A prototypical example of a nonlinear two mass system is an electrical drive with a flexible connection between machine and load, see Section 6. The general nonlinear two mass system with a friction characteristic consisting of a linear term $g\omega_\ell(\cdot)$ (viscous friction) and a bounded nonlinear term $(\mathbf{N}\omega_\ell)(\cdot)$ (Coulomb-friction and Stribeck-effect) is modelled in continuous-time state space form as follows, see [2, Sec. 2],

$$\left. \begin{aligned} \dot{x}(t) &= Ax(t) + b_N [g\omega_\ell(t) + (\mathbf{N}\omega_\ell)(t)] + b[u(t) + \hat{d}(t)], \\ y(t) &= cx(t) \end{aligned} \right\} \quad (2.1)$$

with $c = (c_1, c_2, c_3) \in \mathbb{R}^{1 \times 3}$,

$$A = \begin{bmatrix} -d/J_\ell & k/J_\ell & d/J_\ell \\ -1 & 0 & 1 \\ d/J_d & -k/J_d & -d/J_d \end{bmatrix}, \quad b_N = \begin{pmatrix} -1/J_\ell \\ 0 \\ 0 \end{pmatrix}, \quad b = \begin{pmatrix} 0 \\ 0 \\ 1/J_d \end{pmatrix},$$

where the constants denote

$$\begin{aligned} J_d > 0 &\triangleq \text{moment of inertia (drive-mass) [kgm}^2\text{]}, \\ J_\ell > 0 &\triangleq \text{moment of inertia (load-mass) [kgm}^2\text{]}, \\ d > 0 &\triangleq \text{damping coefficient (elastic shaft) [Nms/rad]}, \\ k > 0 &\triangleq \text{stiffness coefficient (elastic shaft) [Nm/rad]}, \\ g \geq 0 &\triangleq \text{coefficient of the viscous friction [Nms/rad]}. \end{aligned}$$

The state variables are given by $x = (\omega_\ell, \alpha, \omega_d)^T$ with

$$\begin{aligned}\omega_\ell(t) &\triangleq \text{speed of the load at time } t, \\ \alpha(t) &\triangleq \text{angle of twist between the drive and the load at time } t, \\ \omega_d(t) &\triangleq \text{speed of the drive at time } t,\end{aligned}$$

and $\hat{d} \in L^\infty(\mathbb{R} \rightarrow \mathbb{R})$ denotes an arbitrary bounded input disturbance. The inclusion of the disturbance \hat{d} is important, since the controller does not apply a driving torque to the plant directly, but calculates only the desired value for the input. A power converter generates an appropriate current which in turn causes the torque in the machine. The power converter is neglected in the model (2.1) but its influence may be captured by the disturbance \hat{d} .

To include nonlinear effects like friction the nonlinear causal operator

$$\mathbf{N}: C([-h, \infty) \rightarrow \mathbb{R}) \rightarrow L^\infty([0, \infty) \rightarrow \mathbb{R}),$$

is used where $h \geq 0$ quantifies its “memory”. The operator is assumed to satisfy the global boundedness condition

$$\sup \left\{ |(\mathbf{N}\zeta)(t)| \mid t \geq 0, \zeta \in C([-h, \infty) \rightarrow \mathbb{R}) \right\} < \infty, \quad (2.2)$$

and belongs to the following class \mathcal{T} .

Definition 2.1: [Operator class \mathcal{T}]

An operator T is said to be of class \mathcal{T} if, and only if, for some $h \geq 0$, the following hold.

- (i) $T: C([-h, \infty) \rightarrow \mathbb{R}) \rightarrow L^\infty_{\text{loc}}(\mathbb{R}_{\geq 0} \rightarrow \mathbb{R})$.
- (ii) For every $\delta > 0$, there exists $\Delta > 0$ such that, for all $\zeta \in C([-h, \infty) \rightarrow \mathbb{R})$,

$$\sup_{t \in [-h, \infty)} |\zeta(t)| \leq \delta \implies |(T\zeta)(s)| \leq \Delta \text{ for almost all } s \geq 0.$$

- (iii) For all $t \geq 0$, the following hold:

- (a) for all $\zeta, \psi \in C([-h, \infty) \rightarrow \mathbb{R})$,

$$\zeta(\cdot) \equiv \psi(\cdot) \text{ on } [-h, t] \implies (T\zeta)(s) = (T\psi)(s) \text{ for almost all } s \in [0, t];$$

- (b) for all continuous functions $\beta: [-h, t] \rightarrow \mathbb{R}$, there exist $\tau, \delta, c > 0$ such that, for all $\zeta, \psi \in C([-h, \infty) \rightarrow \mathbb{R})$ with $\zeta|_{[-h, t]} = \beta = \psi|_{[-h, t]}$ and $\zeta(s), \psi(s) \in [\beta(t) - \delta, \beta(t) + \delta]$ for all $s \in [t, t + \tau]$,

$$\text{ess-sup}_{s \in [t, t + \tau]} |(T\zeta)(s) - (T\psi)(s)| \leq c \cdot \sup_{s \in [t, t + \tau]} |\zeta(s) - \psi(s)|.$$

Remark 2.2:

- (i) Property (ii) is a bounded-input, bounded-output assumption on the operator T . Property (iii)(a) means causality. Property (iii)(b) is a technical assumption of local Lipschitz type ensuring well-posedness of the closed-loop system.
- (ii) If \mathbf{N} satisfies (2.2) then properties (i) and (ii) are trivially satisfied. We have stated the more general class \mathcal{T} for later purposes. Moreover, the wide range of the operator class \mathcal{T} encompasses – even if restricted by (2.2) – phenomena such as nonlinear friction, relay hysteresis, backlash hysteresis, elastic-plastic hysteresis, Preisach or Prantl hysteresis, see [7]. In view of (2.2), \mathbf{N} cannot model the overall friction characteristic $g\omega_\ell(\cdot) + (\mathbf{N}\omega_\ell)(\cdot)$. For this reason, the friction is split into its linear, unbounded part $g\omega_\ell(\cdot)$ and a nonlinear, bounded operator $(\mathbf{N}\omega_\ell)(\cdot)$ and the linear summand is added to the system matrix A . \diamond

Remark 2.3: [Initial value problem]

Since (2.1) is a functional differential equation, the appropriate initial data are

$$x|_{[-h,0]} = (\omega_\ell^0(\cdot), \alpha^0, \omega_d^0)^T \in C([-h,0] \rightarrow \mathbb{R}) \times \mathbb{R} \times \mathbb{R}. \quad (2.3)$$

By a solution of the initial value problem (2.1), (2.3) on $[-h, \omega)$ we mean a function $x \in C([-h, \omega) \rightarrow \mathbb{R}^3)$, with $0 < \omega \leq \infty$, $x|_{[-h,0]} = x^0$, such that $x|_{[0,\omega)}$ is absolutely continuous and satisfies the differential equations in (2.1) for almost all $t \in [0, \omega)$.

It is shown in [5, Th. 4.2] that the functional initial value problem (2.1), (2.3) has, for any initial data (2.3), a unique solution which can be maximally extended on $[-h, \omega)$, with $0 < \omega \leq \infty$, and if this solution is bounded, then $\omega = \infty$. \diamond

We stress that we will not assume that the entries of A, b_N, b, c, g and the operator \mathbf{N} are known, the modelling and the control is based on structural properties, only. The structural properties are explained in the following.

The concept of relative degree of nonlinear systems, as for example introduced in [6, Sec. 4.1], is essential to design simple feedback controllers for the system. This concept generalizes to functional differential equations (2.1) in the sense that since

$$\dot{y}(t) = c[Ax(t) + b_N [g\omega_\ell(t) + (\mathbf{N}\omega_\ell)(t)]] + \frac{c_3}{J_d} \hat{d}(t) + \frac{c_3}{J_d} u(t),$$

the system (2.1) has relative degree one if, and only if, $c_3 \neq 0$.

As an important consequence of the relative degree one property, (2.1) can be converted into the following normal form.

Remark 2.4: [Byrnes-Isidori normal form]

If the output vector $c = (c_1, c_2, c_3) \in \mathbb{R}^{1 \times 3}$ satisfies $c_3 \neq 0$, then the coordinate transformation

$$\begin{pmatrix} y(t) \\ \omega_\ell(t) \\ \alpha(t) \end{pmatrix} := \begin{bmatrix} c_1 & c_2 & c_3 \\ 1 & 0 & 0 \\ 0 & 1 & 0 \end{bmatrix} \begin{pmatrix} \omega_\ell(t) \\ \alpha(t) \\ \omega_d(t) \end{pmatrix}$$

converts (2.1) into the equivalent system in Byrnes-Isidori normal form

$$\frac{d}{dt} y(t) = a_1 y(t) + a_2 \begin{pmatrix} \omega_\ell(t) \\ \alpha(t) \end{pmatrix} - \frac{c_1}{J_\ell} (\mathbf{N}\omega_\ell)(t) + \frac{c_3}{J_d} \hat{d}(t) + \frac{c_3}{J_d} u(t), \quad (2.4a)$$

$$\frac{d}{dt} \begin{pmatrix} \omega_\ell(t) \\ \alpha(t) \end{pmatrix} = \Lambda \begin{pmatrix} \omega_\ell(t) \\ \alpha(t) \end{pmatrix} + \begin{pmatrix} \frac{d}{c_3 J_\ell} \\ \frac{1}{c_3} \end{pmatrix} y(t) - \begin{pmatrix} \frac{1}{J_\ell} \\ 0 \end{pmatrix} (\mathbf{N}\omega_\ell)(t), \quad (2.4b)$$

where

$$\begin{aligned} a_1 &= \frac{(c_1 - c_3 J_\ell / J_d) d + c_2 J_\ell}{c_3 J_\ell}, \\ a_2 &= \begin{pmatrix} -\frac{d(c_1 c_3 + c_1^2)}{c_3 J_\ell} + \frac{d(c_1 + c_3)}{J_d} - c_2 - \frac{c_1 c_2}{c_3} - \frac{c_1 g}{J_\ell} \\ \frac{c_1 c_3 k - c_1 c_2 d - 2c_2^2 J_\ell}{c_3 J_\ell} + \frac{c_2 d - c_3 k}{J_d} + \frac{c_2^2}{c_3} \end{pmatrix}^T, \\ \Lambda &= \begin{bmatrix} -\frac{d(c_1 + c_3) + c_3 g}{c_3 J_\ell} & \frac{c_3 k - c_2 d}{c_3 J_\ell} \\ -\frac{(c_1 + c_3)}{c_3} & -\frac{c_2}{c_3} \end{bmatrix}. \end{aligned}$$

◇

The Byrnes-Isidori normal form is essential to characterize stability of the zero dynamics (i.e., minimum phase in case of linear systems), see, e.g., [6, Sec. 4.3]. In our concept of functional differential equations this can be generalized as follows.

Definition 2.5: [Asymptotically stable or bounded zero dynamics and ISS]

We say that (2.1) has *asymptotically stable (or bounded) zero dynamics* if, and only if, every solution $(x, y, u) \in C(\mathbb{R}_{\geq 0} \rightarrow \mathbb{R}^3) \times C(\mathbb{R}_{\geq 0} \rightarrow \mathbb{R}) \times C(\mathbb{R}_{\geq 0} \rightarrow \mathbb{R})$ of (2.1) with $y \equiv 0$ satisfies $\lim_{t \rightarrow \infty} x(t) = 0$ and $\lim_{t \rightarrow \infty} u(t) = 0$ (or $x \in L^\infty(\mathbb{R}_{\geq 0} \rightarrow \mathbb{R}^3)$ and $u \in L^\infty(\mathbb{R}_{\geq 0} \rightarrow \mathbb{R})$).

We say that (2.1) is *input-to-state stable* if, and only if, for every $u \in L^\infty(\mathbb{R}_{\geq 0} \rightarrow \mathbb{R})$ and initial condition (2.3) there exists a solution x on $[0, \omega)$ for some $\omega > 0$, and every solution satisfies $\omega = \infty$ and $x \in L^\infty(\mathbb{R}_{\geq 0} \rightarrow \mathbb{R})$. ◇

Remark 2.6: [Stability properties of (2.1)]

If the output vector c in (2.1) is considered as a design parameter, then independently of the remaining parameters in (2.1), the following relationships of the parameters are essential for the stability properties of the model.

$$c_3 > 0, \quad c_2 \geq 0, \quad c_1 > -c_3. \quad (2.5)$$

A straightforward calculation gives

$$(2.5) \implies \text{spec}(\Lambda) \subset \mathbb{C}_-$$

and

$$\text{spec}(\Lambda) \subset \mathbb{C}_- \implies (2.4b) \text{ is input } y \text{ to state } (\omega_\ell, \alpha) \text{ stable,}$$

and also

$$\text{spec}(\Lambda) \subset \mathbb{C}_- \implies \begin{array}{l} (2.4) \text{ has bounded zero dynamics or, if } \mathbf{N} \equiv 0, \\ \text{has asymptotically stable zero dynamics.} \end{array}$$

The form (2.4) also shows that, provided (2.5) holds, the system (2.1) is practically high-gain stabilizable in the sense that for any $\varepsilon > 0$ there exists $\kappa > 0$ sufficiently large so that $u(t) = -\kappa y(t)$ applied to (2.1) yields $\limsup_{t \rightarrow \infty} |y(t)| \leq \varepsilon$. To prove this, differentiate the Lyapunov function $(y, \omega_\ell, \alpha) \mapsto y^2 + (\omega_\ell, \alpha)P(\omega_\ell, \alpha)^T$, where $P > 0$ denotes the unique solution of $\Lambda^T P + P\Lambda = -I_2$, along the solution and use obvious estimates. ◇

We are now in a position to rewrite (2.1), under the assumption (2.5), to an equivalent functional differential equation in one variable y only. This is essential for applying the funnel controller as will be done in Section 5.

Proposition 2.7: [System (2.1) in one variable]

Suppose (2.5) holds. Then (2.1) with initial data (2.3) may be written, for some $\mathbf{T} \in \mathcal{T}$ and $p \in L^\infty(\mathbb{R}_{\geq 0} \rightarrow \mathbb{R})$, as

$$\frac{d}{dt} y(t) = (\mathbf{T}y)(t) + p(t) + \frac{c_3}{J_d} u(t), \quad y|_{[-h, 0]} = c(\omega_\ell^0(\cdot), \alpha^0, \omega_d^0)^T. \quad (2.6)$$

Proof: Consider (2.4) and set

$$\begin{aligned} \mathbf{T}_1 & : L_{\text{loc}}^\infty(\mathbb{R}_{\geq 0} \rightarrow \mathbb{R}) \rightarrow L_{\text{loc}}^\infty(\mathbb{R}_{\geq 0} \rightarrow \mathbb{R}), \quad \zeta(\cdot) \mapsto \int_0^\cdot e^{\Lambda(\cdot-s)} \zeta(s) ds, \\ p(\cdot) & := a_2 e^\Lambda \cdot \begin{pmatrix} \omega_\ell^0(0) \\ \alpha^0 \end{pmatrix} + a_2 \left(\mathbf{T}_1 \begin{pmatrix} -1 \\ 0 \end{pmatrix} (\mathbf{N}\omega_\ell) \right) (\cdot) - \frac{c_2}{J_\ell} (\mathbf{N}\omega_\ell)(\cdot) + \frac{c_3}{J_d} \hat{d}(\cdot), \\ (\mathbf{T}y)(\cdot) & := a_1 y(\cdot) + a_2 \left(\mathbf{T}_1 \begin{pmatrix} d \\ \frac{1}{c_3} \end{pmatrix} y \right) (\cdot). \end{aligned}$$

Invoking (2.2), Remark 2.6 and $\hat{d} \in L^\infty(\mathbb{R} \rightarrow \mathbb{R})$, it follows from [4, Subsection 4.1] that $\mathbf{T}_1 \in \mathcal{T}$, $p \in L^\infty(\mathbb{R}_{\geq 0} \rightarrow \mathbb{R})$, and also $\mathbf{T} \in \mathcal{T}$. Hence we may apply variation of constants to equation (2.4b) and substituting this into equation (2.4a) yields, with the above notation, equation (2.6). \square

We will see the importance of the functional differential equation (2.6) when we introduce the funnel controller (4.15). Loosely speaking, since (2.1) has exponentially stable zero dynamics if $\mathbf{N} \equiv 0$ (see Remark 2.6), the operator \mathbf{T} belongs to the class \mathcal{T} and so $(\mathbf{T}y)(\cdot)$ is bounded if $y(\cdot)$ is bounded. This allows to apply the funnel controller as in [4].

3. THE CONTROL OBJECTIVES

The control objectives are captured by the concept of funnel control as introduced by [4]: A prespecified performance funnel

$$\mathcal{F}_\varphi := \{(t, e) \in \mathbb{R}_{\geq 0} \times \mathbb{R} \mid \varphi(t) |e| < 1\}$$

is associated with a function φ (the reciprocal of which determines the funnel boundary) of the class

$$\Phi_\lambda := \{\varphi \in W^{1,\infty}(\mathbb{R}_{\geq 0}, \mathbb{R}_{\geq 0}) \mid \varphi(0) = 0, \quad \varphi(s) > 0 \text{ for all } s > 0 \text{ and } \liminf_{s \rightarrow \infty} \varphi(s) > \lambda^{-1}\},$$

where $\lambda > 0$ describes the “ultimate width” of the funnel, see Figure 3.3.

We are now in a position to describe the control objective: the aim is to design a feedback strategy which ensures with reference to Figure 1.2, for every reference signal $y_{\text{ref}} \in W^{1,\infty}(I \rightarrow \mathbb{R})$, i.e. bounded signals with essentially bounded derivative, and every disturbance signal $\hat{d} \in L^\infty(\mathbb{R} \rightarrow \mathbb{R})$,

- (i) the output error $e = \hat{y} - y_{\text{ref}}$ evolves within the funnel;
- (ii) the output error $e(t)$ is, for prespecified time $\tau > 0$ onwards, smaller than a prespecified tracking accuracy $\lambda_\tau > 0$;
- (iii) all signals in the closed-loop system are bounded;
- (iv) if the closed-loop system is “close” to a steady state for “large” t , then the output error e is “small” for “large” t ;
- (v) oscillations in the elastic shaft are damped;
- (vi) any disturbance $\hat{d} \in L^\infty(\mathbb{R} \rightarrow \mathbb{R})$ is rejected.

The control objectives (i) and (ii) are captured by the funnel controller, see Sub-section 4.3. For example, if φ is chosen as the function $t \mapsto \min\{t/\tau, 1\}/\lambda_\tau$, then evolution within the funnel ensures that the prescribed tracking accuracy $\lambda_\tau > 0$ is achieved within the prescribed time $\tau > 0$. Objective (iv) is addressed by invoking a PI-controller in series with the funnel controller, see Sub-section 4.2. Objective (v) is taken care of by introducing a high pass filter, see Sub-section 4.1. The objective (iii) is addressed by the conjunction of all three controllers.

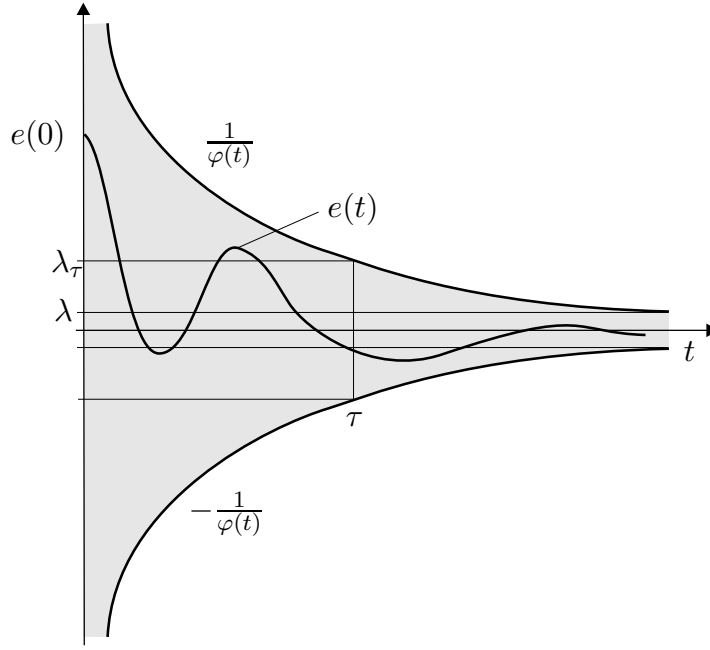


Fig. 3.3. Prescribed performance funnel \mathcal{F}_φ

4. THE CONTROLLERS

In this section we conjunct the nominal system (2.1) with the high pass filter, the PI-controller and both of them. For all possible conjunctions it is shown that the augmented systems inherit the properties of the nominal system in the sense that it allows to write the input-output systems in form of a scalar functional differential equation of the form (2.6).

A. High pass filter (HPF)

We conjunct – see also Figure 1.2 – the high-pass filter (HPF)

$$\dot{\eta}(t) = -\frac{1}{T}\eta(t) + \alpha(t), \quad \eta(0) = 0, \quad (4.7)$$

for a design parameter $T > 0$ with the output y by defining the new output

$$\hat{y}(t) = y(t) - \frac{c_2}{T}\eta(t). \quad (4.8)$$

The effect of the high-pass filter is, loosely spoken, to detect in the new output whether the angle of twist $\alpha(\cdot)$ oscillates or not. If $\alpha(\cdot) \approx \text{const.}$, then

$$\hat{y}(\cdot) \approx y(\cdot) - \frac{c_2}{T}T \text{ const.} = c_1\omega_\ell(\cdot) + c_3\omega_d(\cdot),$$

and so $\alpha(\cdot)$ pays no contribution in the new output $\hat{y}(\cdot)$. If the signal $\alpha(\cdot)$ contains oscillations as high frequencies, they pass the filter with nearly no attenuation, and since the input of the filter passes the feed-through path without any delay, every change of the input is visible in the output \hat{y} immediately.

Note that although (4.7) describes a low pass filter of first order we call it high pass filter since the overall dynamics from the input $\alpha(\cdot)$ to the output $\hat{y}(\cdot)$ behave like a high pass filter.

In the following proposition we show that the conjunction of the nominal system (2.1) with the high-pass filter (4.7) and new output (4.8) can also be described as a scalar functional differential equation similar to (2.6).

Proposition 4.1: [(2.1) & (HPF)]

Suppose (2.5) holds. Then the nominal system (2.1) with initial data (2.3) in conjunction with the high-pass filter (4.7), (4.8) for $T > 0$ may be written, for some $\hat{\mathbf{T}} \in \mathcal{T}$ and $\hat{p} \in L^\infty(\mathbb{R}_{\geq 0} \rightarrow \mathbb{R})$, as

$$\frac{d}{dt} \hat{y}(t) = (\hat{\mathbf{T}}\hat{y})(t) + \hat{p}(t) + \frac{c_3}{J_d} u(t), \quad \hat{y}|_{[-h,0]} = c \left(\omega_\ell^0(\cdot), \alpha^0, \omega_d^0 \right)^T. \quad (4.9)$$

Proof: The augmented input-output system (2.1), (4.7), (4.8) with initial data (2.3) becomes

$$\left. \begin{aligned} \frac{d}{dt} \hat{x}(t) &= \hat{A} \hat{x}(t) + b_N [g \hat{x}_1(t) + (\mathbf{N}\hat{x}_1)(t)] + \hat{b} [u(t) + \hat{d}(t)], & \hat{x}(0) &= \hat{x}^0 \\ \hat{y}(t) &= \hat{c} \hat{x}(t) \end{aligned} \right\} \quad (4.10)$$

with

$$\hat{A} = \begin{bmatrix} & 0 & & \\ A & 0 & & \\ & 0 & & \\ 0 & 1 & 0 & -1/T \end{bmatrix}, \quad A \text{ as in (2.1),}$$

$$\hat{b}_N = \begin{pmatrix} b_N \\ 0 \end{pmatrix} = \begin{pmatrix} -1/J_\ell \\ 0 \\ 0 \\ 0 \end{pmatrix}, \quad \hat{b} = \begin{pmatrix} b \\ 0 \end{pmatrix} = \begin{pmatrix} 0 \\ 0 \\ 1/J_d \\ 0 \end{pmatrix}, \quad \hat{c} = \begin{pmatrix} c_1 \\ c_2 \\ c_3 \\ -c_2/T \end{pmatrix}^T,$$

$$\hat{x}(t) = \begin{pmatrix} x(t) \\ \eta(t) \end{pmatrix} = (\omega_\ell(t), \alpha(t), \omega_d(t), \eta(t))^T, \quad \hat{x}^0 = \begin{pmatrix} x^0 \\ 0 \end{pmatrix}.$$

The coordinate transformation

$$\begin{pmatrix} \hat{y}(t) \\ \omega_\ell(t) \\ \alpha(t) \\ \eta(t) \end{pmatrix} := \begin{bmatrix} c_1 & c_2 & c_3 & -c_2/T \\ 1 & 0 & 0 & 0 \\ 0 & 1 & 0 & 0 \\ 0 & 0 & 0 & 1 \end{bmatrix} \begin{pmatrix} \omega_\ell(t) \\ \alpha(t) \\ \omega_d(t) \\ \eta(t) \end{pmatrix}$$

converts (4.10) into the equivalent system in Byrnes-Isidori normal form

$$\left. \begin{aligned} \frac{d}{dt} \hat{y}(t) &= \hat{a}_1 \hat{y}(t) + \hat{a}_2 \begin{pmatrix} \omega_\ell(t) \\ \alpha(t) \\ \eta(t) \end{pmatrix} - \frac{c_1}{J_\ell} (\mathbf{N}\omega_\ell)(t) + \frac{c_3}{J_d} \hat{d}(t) + \frac{c_3}{J_d} u(t), \\ \frac{d}{dt} \begin{pmatrix} \omega_\ell(t) \\ \alpha(t) \\ \eta(t) \end{pmatrix} &= \hat{\Lambda} \begin{pmatrix} \omega_\ell(t) \\ \alpha(t) \\ \eta(t) \end{pmatrix} + \begin{pmatrix} \frac{d}{c_3 J_\ell} \\ \frac{1}{c_3} \\ 0 \end{pmatrix} \hat{y}(t) - \begin{pmatrix} \frac{1}{J_\ell} \\ 0 \\ 0 \end{pmatrix} (\mathbf{N}\omega_\ell)(t), \end{aligned} \right\} \quad (4.11)$$

where

$$\begin{aligned} \hat{a}_1 &= \frac{(c_1 J_d - c_3 J_\ell) d}{c_3 J_d J_\ell} + \frac{c_2}{c_3}, \\ \hat{a}_2 &= \begin{pmatrix} -\frac{(c_1 c_3 + c_1^2) d}{c_3 J_\ell} - \frac{c_2 c_3 + c_1 c_2}{J_d} + \frac{(c_1 + c_3) d}{J_d} - \frac{c_1 g}{J_\ell} \\ \frac{(c_1 J_d - c_3 J_\ell) k}{J_d J_\ell} + \frac{c_2 (dT - J_d)}{J_d T} - \frac{c_1 c_2 d}{c_3 J_\ell} - \frac{c_2^2}{c_3} \\ \frac{c_1 c_2 d}{c_3 J_\ell T} + \frac{c_2^2}{c_3 T} - \frac{c_2 d}{J_d T} + \frac{c_2}{T^2} \end{pmatrix}^T, \\ \hat{\Lambda} &= \begin{bmatrix} -\frac{d(c_1 + c_3) + c_3 g}{c_3 J_\ell} & \frac{c_3 k - c_2 d}{c_3 J_\ell} & \frac{c_2 d}{c_3 T J_\ell} \\ \frac{-(c_1 + c_3)}{c_3} & -\frac{c_2}{c_3} & \frac{c_2}{c_3 T} \\ 0 & 1 & -\frac{1}{T} \end{bmatrix}. \end{aligned}$$

To show that $\text{spec } \hat{\Lambda} \subset \mathbb{C}_-$, calculate

$$\begin{aligned} \det(\lambda I_3 - c_3 T J_\ell \hat{\Lambda}) &= \lambda^3 + [c_3 J_\ell + (c_1 + c_3)dT + c_3 gT + c_2 T J_\ell] \lambda^2 \\ &\quad + [c_3 J_\ell T (c_1 + c_3)(d + kT) + c_3 g J_\ell T (c_2 T + c_3)] \lambda + c_3^2 k J_\ell^2 T^2 (c_1 + c_3). \end{aligned}$$

Since (2.5) yields that all coefficients of the above polynomial are positive and

$$\begin{aligned} [c_3 J_\ell + (c_1 + c_3)dT + c_3 gT + c_2 T J_\ell] \cdot [c_3 J_\ell T (c_1 + c_3)(d + kT) + c_3 g J_\ell T (c_2 T + c_3)] \\ - c_3^2 k J_\ell^2 T^2 (c_1 + c_3) > 0, \end{aligned}$$

it follows from the Hurwitz conditions (see, e.g. [3, p. 23]) that $\text{spec } \hat{\Lambda} \subset \mathbb{C}_-$. Now the remainder of the proof is completely analogous to the proof of Proposition 2.7. \square

B. PI-controller (PI)

It has been observed in [9] that the application of the funnel controller, which will be introduced in Sub-section 4.3, alone exhibits a nonzero error in the steady state. To overcome this drawback we introduce – see also Figure 1.2 – a PI-controller as a pre-compensator to (2.1). The PI-controller has the form

$$\left. \begin{aligned} \frac{d}{dt} \xi(t) &= v(t), & \xi(0) &= 0 \\ u(t) &= k_I \xi(t) + k_P v(t), \end{aligned} \right\} \quad (4.12)$$

with design parameters $k_I, k_P > 0$.

It is easy to see, that the control error vanishes, if a steady state is attained, i.e. $\lim_{t \rightarrow \infty} \frac{d}{dt} \xi(t) = 0$. From (4.12) it follows that a steady state for ξ is equivalent to $\lim_{t \rightarrow \infty} v(t) = 0$, and thus a proportional error feedback (defined in due course in Sub-section 4.3) of the form $v(t) = -\kappa(t)e(t)$ yields $\lim_{t \rightarrow \infty} e(t) = 0$, provided that $\limsup_{t \rightarrow \infty} \kappa(t) > 0$.

Next we will show that the nominal system (2.1) in conjunction with the PI-controller (4.12) can also be described as a scalar functional differential equation similar to (2.6).

Proposition 4.2: [(2.1) & (PI)]

The nominal system (2.1) with initial data (2.3) in conjunction with the PI-controller (4.12), may be written, for some $\hat{\mathbf{T}} \in \mathcal{T}$ and $\hat{p} \in L^\infty(\mathbb{R}_{\geq 0} \rightarrow \mathbb{R})$, as

$$\frac{d}{dt} y(t) = (\hat{\mathbf{T}}y)(t) + \hat{p}(t) + \frac{c_3 k_P}{J_d} v(t), \quad y|_{[-h, 0]} = c(\omega_\ell^0(\cdot), \alpha^0, \omega_d^0)^T.$$

The proof of Proposition 4.2 is postponed since it is a simplification of the proof of the next proposition.

Next we conjunct the nominal system (2.1) with high-pass filter (4.7), (4.8) and the PI-controller (4.12) and show that the structural properties of (2.1) remain.

Proposition 4.3: [(2.1) & (HPF-PI)]

Suppose (2.5) holds. Then the nominal system (2.1) with initial data (2.3) in conjunction with the high-pass filter (4.7), (4.8) and the PI-controller (4.12), i.e. the input-output system (4.13), may be written, for some $\hat{\mathbf{T}} \in \mathcal{T}$ and $\hat{p} \in L^\infty(\mathbb{R}_{\geq 0} \rightarrow \mathbb{R})$, as

$$\frac{d}{dt} \hat{y}(t) = (\hat{\mathbf{T}}\hat{y})(t) + \hat{p}(t) + \frac{c_3 k_P}{J_d} v(t), \quad \hat{y}|_{[-h,0]} = c(\omega_\ell^0(\cdot), \alpha^0, \omega_d^0)^T.$$

Proof: The closed loop system (2.1), (4.12), (4.7), (4.8) is given by

$$\left. \begin{aligned} \frac{d}{dt} \begin{pmatrix} \omega_\ell(t) \\ \alpha(t) \\ \omega_d(t) \\ \eta(t) \\ \xi(t) \end{pmatrix} &= \begin{bmatrix} -d/J_\ell - g/J_\ell & k/J_\ell & d/J_\ell & 0 & 0 \\ -1 & 0 & 1 & 0 & 0 \\ d/J_d & -k/J_d & -d/J_d & 0 & k_I/J_d \\ 0 & 1 & 0 & -1/T & 0 \\ 0 & 0 & 0 & 0 & 0 \end{bmatrix} \begin{pmatrix} \omega_\ell(t) \\ \alpha(t) \\ \omega_d(t) \\ \eta(t) \\ \xi(t) \end{pmatrix} \\ &+ \begin{pmatrix} -1/J_\ell \\ 0 \\ 0 \\ 0 \\ 0 \end{pmatrix} (\mathbf{N}\omega_\ell)(t) + \begin{pmatrix} 0 \\ 0 \\ k_P/J_d \\ 0 \\ 1 \end{pmatrix} v(t) + \begin{pmatrix} 0 \\ 0 \\ 1/J_d \\ 0 \\ 0 \end{pmatrix} \hat{d}(t). \end{aligned} \right\} \quad (4.13)$$

The coordinate transformation

$$\begin{pmatrix} \hat{y}(t) \\ \omega_\ell(t) \\ \alpha(t) \\ \eta(t) \\ \zeta(t) \end{pmatrix} := \begin{bmatrix} c_1 & c_2 & c_3 & -c_2/T & 0 \\ 1 & 0 & 0 & 0 & 0 \\ 0 & 1 & 0 & 0 & 0 \\ 0 & 0 & 0 & 1 & 0 \\ c_1 & c_2 & c_3 & -c_2/T & -c_3 k_P/J_d \end{bmatrix} \begin{pmatrix} \omega_\ell(t) \\ \alpha(t) \\ \omega_d(t) \\ \eta(t) \\ \xi(t) \end{pmatrix}$$

converts (4.13) to the equivalent system in Byrnes-Isidori normal form

$$\left. \begin{aligned} \frac{d}{dt} \hat{y}(t) &= \tilde{a}_1 \hat{y}(t) + \tilde{a}_2 \begin{pmatrix} \omega_\ell(t) \\ \alpha(t) \\ \eta(t) \\ \zeta(t) \end{pmatrix} - \frac{c_1}{J_\ell} (\mathbf{N}\omega_\ell)(t) + \frac{c_3}{J_d} [k_P v(t) + \hat{d}(t)] \\ \frac{d}{dt} \begin{pmatrix} \omega_\ell(t) \\ \alpha(t) \\ \eta(t) \\ \zeta(t) \end{pmatrix} &= \tilde{\Lambda} \begin{pmatrix} \omega_\ell(t) \\ \alpha(t) \\ \eta(t) \\ \zeta(t) \end{pmatrix} + \tilde{a}_4 \hat{y}(t) - \begin{pmatrix} 1/J_\ell \\ 0 \\ 0 \\ c_1/J_\ell \end{pmatrix} (\mathbf{N}\omega_\ell)(t) + \begin{pmatrix} 0 \\ 0 \\ 0 \\ c_3/J_d \end{pmatrix} \hat{d}(t), \end{aligned} \right\} \quad (4.14)$$

where

$$\begin{aligned} \tilde{a}_1 &= \frac{c_1 d}{c_3 J_\ell} + \frac{c_2}{c_3} - \frac{d}{J_d} + \frac{k_I}{k_P} \\ \tilde{a}_2 &= \begin{pmatrix} -\frac{c_1 d}{J_\ell} - c_2 - \frac{c_1 c_2}{c_3} + \frac{(c_1 + c_3)d}{J_d} - \frac{c_1^2 d}{c_3 J_\ell} - \frac{c_1 g}{J_\ell} \\ \frac{c_1 k}{J_\ell} - \frac{c_3 k}{J_d} - \frac{c_2}{T} - \frac{c_1 c_2 d}{c_3 J_\ell} - \frac{c_2^2}{c_3} + \frac{c_2 d}{J_d} \\ c_2 \cdot \left(\frac{c_1 d}{c_3 J_\ell T} + \frac{c_2}{c_3 T} - \frac{d}{J_d T} + \frac{1}{T^2} \right) \\ -\frac{k_I}{k_P} \end{pmatrix}^T \end{aligned}$$

$$\tilde{a}_4 = (d/(J_\ell c_3), 1/c_3, 0, \tilde{a}_1)^T$$

$$\tilde{\Lambda} = \begin{bmatrix} -\frac{d(c_1+c_3)+c_3g}{c_3J_\ell} & \frac{c_3k-c_2d}{c_3J_\ell} & \frac{c_2d}{c_3TJ_\ell} & 0 \\ \frac{-(c_1+c_3)}{c_3} & -\frac{c_2}{c_3} & \frac{c_2}{c_3T} & 0 \\ 0 & 1 & \frac{-1}{T} & 0 \\ & \tilde{a}_2 & & \end{bmatrix}$$

Since $\text{spec } \tilde{\Lambda} = \text{spec } \hat{\Lambda} \cup \{-k_I/k_P\}$, the remainder of the proof is completely analogous to the proof of Proposition 2.7. \square

Proof of Proposition 4.2: The proof of Proposition 4.2 is a simplification of the proof of Proposition 4.3. The closed-loop system (2.1), (4.12) is (4.13) with missing η component. To this system you may apply the coordinate transformation

$$\begin{pmatrix} \hat{y}(t) \\ \omega_\ell(t) \\ \alpha(t) \\ \zeta(t) \end{pmatrix} := \begin{bmatrix} c_1 & c_2 & c_3 & 0 \\ 1 & 0 & 0 & 0 \\ 0 & 1 & 0 & 0 \\ c_1 & c_2 & c_3 & -c_3k_P/J_d \end{bmatrix} \begin{pmatrix} \omega_\ell(t) \\ \alpha(t) \\ \omega_d(t) \\ \xi(t) \end{pmatrix}$$

and end up with a similar Byrnes-Isidori normal form as in (4.14), again η component is missing, and the matrix $\tilde{\Lambda}$ is replaced by

$$\bar{\Lambda} = \begin{bmatrix} -\frac{d(c_1+c_3)+c_3g}{c_3J_\ell} & \frac{c_3k-c_2d}{c_3J_\ell} & 0 \\ \frac{-(c_1+c_3)}{c_3} & -\frac{c_2}{c_3} & 0 \\ & \bar{a}_2 & \end{bmatrix}, \quad \bar{a}_2 = \begin{pmatrix} -\frac{c_1d}{J_\ell} - c_2 - \frac{c_1c_2}{c_3} + \frac{(c_1+c_3)d}{J_d} - \frac{c_1^2d}{c_3J_\ell} - \frac{c_1g}{J_\ell} \\ \frac{c_1k}{J_\ell} - \frac{c_3k}{J_d} - \frac{c_1c_2d}{c_3J_\ell} - \frac{c_2^2}{c_3} + \frac{c_2d}{J_d} \\ -\frac{k_I}{k_P} \end{pmatrix}^T.$$

Since

$$\text{spec } \bar{\Lambda} = \text{spec} \begin{bmatrix} -\frac{d(c_1+c_3)+c_3g}{c_3J_\ell} & \frac{c_3k-c_2d}{c_3J_\ell} \\ \frac{-(c_1+c_3)}{c_3} & -\frac{c_2}{c_3} \end{bmatrix} \cup \{-k_I/k_P\} = \text{spec } \Lambda \cup \{-k_I/k_P\},$$

for Λ as in (2.4b). Now the remainder of the proof is completely analogous to the proof of Proposition 2.7. \square

C. Funnel controller (FC)

Finally, we introduce the funnel controller in conjunction with the high-pass filter (4.7), (4.8) and/or the PI-controller (4.12): set, for $\lambda > 0$ and $\varphi \in \Phi_\lambda$,

$$\left. \begin{aligned} v(t) &= -\kappa(t) e(t), \\ \kappa(t) &= \frac{1}{1-\varphi(t)|e(t)|}. \end{aligned} \right\} \quad (4.15)$$

The intuition of the funnel controller (4.15) with $e(t) = y(t) - y_{\text{ref}}(t)$ and $y_{\text{ref}} \in W^{1,\infty}(\mathbb{R}_{\geq 0} \rightarrow \mathbb{R})$ applied to a nominal system (2.1) satisfying (2.5) is as follows. By Proposition 2.7, the closed-loop system (2.1), (4.15), $e(t) = y(t) - y_{\text{ref}}(t)$ may be written as

$$\left. \begin{aligned} \frac{d}{dt} e(t) &= -\frac{c_3}{J_d} \kappa(t) e(t) + \psi(t), \\ \kappa(t) &= \frac{1}{1-\varphi(t)|e(t)|}, \\ \psi(t) &= (\mathbf{T}y)(t) + p(t) - \dot{y}_{\text{ref}}(t). \end{aligned} \right\} \quad (4.16)$$

It follows from Proposition 2.7 and $y_{\text{ref}} \in W^{1,\infty}(\mathbb{R} \rightarrow \mathbb{R})$, and ignoring problems of finite escape time for the moment, that $\psi \in L^\infty(\mathbb{R} \rightarrow \mathbb{R})$. Now, if $(t, e(t))$ approaches the funnel boundary, then by construction $\kappa(t)$ becomes sufficiently large so that the first equation in (4.16) precludes boundary contact and e will stay within the funnel.

In the following section we will give a precise proof of this statement and also show that it holds for the various conjunctions with PI-controller and/or high pass filter.

5. MAIN RESULT

We are now in a position to show the main result of this paper. The control objectives (i)-(vi) of Section 3 will be addressed by the conjunction of the high pass filter (4.7), PI-controller (4.12) and funnel controller (4.15). Note the simplicity of all three controllers and that they do not depend on special data of the system but only on structural assumptions; the assumption (2.5) which bounded zero dynamics (minimum phase in the linear case) the model and positivity of the high frequency gain, see Remark 2.6.

Theorem 5.1:

Suppose (2.5) holds. Let a funnel \mathcal{F}_φ be determined by $\varphi \in \Phi_\lambda$ for $\lambda > 0$. Then the application of each of the following controllers

(FC): funnel controller (4.15), $e(t) = y(t) - y_{\text{ref}}(t)$, $v(t) = u(t)$

(HPF-FC): high-pass filter (4.7), funnel controller (4.15), $e(t) = \hat{y}(t) - y_{\text{ref}}(t)$, $v(t) = u(t)$

(PI-FC): funnel controller (4.15), $e(t) = y(t) - y_{\text{ref}}(t)$, PI-controller (4.12), $k_I, k_P > 0$

(HPF-PI-FC): high-pass filter (4.7), funnel controller (4.15), $e(t) = \hat{y}(t) - y_{\text{ref}}(t)$, PI-controller (4.12), $k_I, k_P > 0$

in conjunction with any nominal system (2.1) yields, for arbitrary initial data

$x|_{[-h,0]} = (\omega_\ell^0(\cdot), \alpha^0, \omega_d^0)^T \in C([-h,0] \rightarrow \mathbb{R}) \times \mathbb{R} \times \mathbb{R}$ and arbitrary reference signal $y_{\text{ref}} \in W^{1,\infty}(I \rightarrow \mathbb{R})$, a closed-loop initial value problem which has a solution, every solution has a maximal extension on $[0, \infty)$, every solution component is bounded on $[0, \infty)$, and moreover:

- (i) there exists $\varepsilon \in (0, 1)$ such that, for all $t \geq 0$, $\varphi(t)|e(t)| \leq 1 - \varepsilon$;
- (ii) if the PI-controller is invoked, that means (PI-FC) or (HPF-PI-FC) is considered, then we have, for all $t \geq 0$, $|e(t)| < |\dot{\xi}(t)|$. \diamond

Note that (i) ensures that the error inside the funnel is bounded away from the funnel boundary; and (ii) ensures that the error is smaller than the derivative of the ξ variable of the PI-controller and so the error tends to zero if the system tends to a steady state.

Proof of Theorem 5.1: We consider the four different control schemes.

(FC): By Proposition 2.7, the input-output system (2.1) may be written as (2.6) and the latter satisfies all assumptions required in [4, Th. 7] so that the application of the funnel controller (4.15), $e(t) = \hat{y}(t) - y_{\text{ref}}(t)$ ensures all - apart from (ii) - assertions claimed in the theorem.

(HPF-FC): To see this proof, use Proposition 4.1 and argue as in (FC) above.

(PI-FC): To see this proof, use Proposition 4.2 and argue as in (FC) above.

(HPF-PI-FC): To see this proof, use Proposition 4.3 and argue as in (FC) above.

Finally, assertion (ii), in case of (PI-FC) or (HPF-PI-FC), follows from $\dot{\xi}(t) = -\kappa(t)e(t)$ and the fact that $\kappa(t) > 1$. \square

Note that the controller (4.7), (4.12), (4.15) tolerates output measurement noise n as depicted in Figure 1.2. The noise $n \in W^{1,\infty}(\mathbb{R}_{\geq 0} \rightarrow \mathbb{R})$ is viewed as the reference signal y_{ref} since $e = \hat{y}(t) - y_{\text{ref}} + n$. Hence, in the presence of measurement noise a bound for its amplitude should be known so that the width $\lambda > 0$ of the funnel can be chosen greater than this bound; otherwise the controller ensures only that \hat{y} is “following” the noise.

The fundamental assumption in Theorem 5.1 is that the system (2.1) has relative degree one. This allows to use the simple feedback control strategy (4.15) in conjunction with the high pass filter (4.7), (4.8) and the PI-controller (4.12). For many two mass system applications the control objective is to control the speed of the load ω_ℓ , and this means that the system has relative degree two. In terms of our model, the vector c in (2.1) would be replaced by

$$(c_1, c_2, c_3) = (1, 0, 0), \quad \text{i.e. } y = \omega_\ell.$$

A suitable relative degree two controller would be much more involved since it would invoke back-stepping, see [5], or derivative feedback.

However, the controllers considered in Theorem 5.1 are not too bad if the system is “close” to a steady state. In the following corollary we will give an explicit formula for $\omega_\ell(t) - \omega_{\text{ref}}(t)$, that is the difference of the speed of the load and a prespecified reference trajectory ω_{ref} . It shows how this difference is related to other system states, depending on which control scheme is used.

Corollary 5.2: [Tracking of the load]

Suppose (2.5) holds. Let $\omega_{\text{ref}} \in W^{1,\infty}(I \rightarrow \mathbb{R})$ be a prespecified reference signal for the speed of the load. Let a funnel \mathcal{F}_φ be determined by $\varphi \in \Phi_\lambda$ and $\lambda > 0$. Then the application of the four controllers investigated in Theorem 5.1 for

$$y_{\text{ref}}(\cdot) := (c_1 + c_3)\omega_{\text{ref}}(\cdot) \tag{5.17}$$

to any system (2.1) yields, for arbitrary initial data $x|_{[-h,0]} = (\omega_\ell^0(\cdot), \alpha^0, \omega_d^0)^T \in C([-h, 0] \rightarrow \mathbb{R}) \times \mathbb{R} \times \mathbb{R}$, a closed-loop initial value problem with properties described in Theorem 5.1 and moreover the difference between the load and the load reference signal satisfies, for all $t \geq 0$,

$$\text{(FC): } \omega_\ell(t) - \omega_{\text{ref}}(t) = \frac{1}{c_1 + c_3} [e(t) - c_2\alpha(t) - c_3\dot{\alpha}(t)],$$

$$\text{(HPF-FC): } \omega_\ell(t) - \omega_{\text{ref}}(t) = \frac{1}{c_1 + c_3} [e(t) - c_2\alpha(t) - c_3\dot{\alpha}(t) + \frac{c_2}{T}\eta(t)],$$

$$\text{(PI-FC): } \omega_\ell(t) - \omega_{\text{ref}}(t) = \frac{1}{c_1 + c_3} [-\kappa(t)^{-1}\dot{\xi}(t) - c_2\alpha(t) - c_3\dot{\alpha}(t)],$$

$$\text{(HPF-PI-FC): } \omega_\ell(t) - \omega_{\text{ref}}(t) = \frac{1}{c_1 + c_3} [-\kappa(t)^{-1}\dot{\xi}(t) - c_2\alpha(t) - c_3\dot{\alpha}(t) + \frac{c_2}{T}\eta(t)].$$

Proof:

We consider the four different control schemes as in Theorem 5.1 and leave out the argument t for simplicity. Then (2.1) and (5.17) give

$$y - y_{\text{ref}} = (c_1 + c_3)(\omega_\ell - \omega_{\text{ref}}) + c_2\alpha + c_3(\omega_d - \omega_\ell)$$

and, in view of $\dot{\alpha} = \omega_d - \omega_\ell$, the statement for (FC) follows.

Next consider (HPF-FC) which gives

$$\hat{y} - y_{\text{ref}} = (c_1 + c_3)(\omega_\ell - \omega_{\text{ref}}) + c_2\alpha + c_3(\omega_d - \omega_\ell) - \frac{c_2}{T}\eta$$

and, in view of $\dot{\alpha} = \omega_d - \omega_\ell$ and (4.7), the statement follows.

The statement (PI-FC) follows from the statement (FC) by substituting $e = -\kappa^{-1} \dot{\xi}$, which is a consequence of the first equation in (4.12) in conjunction with $v = e$, into the statement (FC).

Finally, to show the statement (HPF-PI-FC), substitute $e = -\kappa^{-1} \dot{\xi}$ into the statement (HPF-FC). This completes the proof of the corollary. \square

Corollary 5.2 allows to decide which controller is appropriate for a given control objective. Since the control error $e(t)$ is bounded by the funnel, its maximum value can be made arbitrarily small – at least theoretically if no measurement noise is present – by a small funnel. For this reason, assume $e(t)$ is “small”, that means within an “acceptable” range. In the case (FC), the deviation $\omega_\ell(t) - \omega_{\text{ref}}(t)$ depends on the angle of twist and its derivative and the small $e(t)$. Hence, for the ideal situation $\omega_\ell(t) - \omega_{\text{ref}}(t) \equiv 0$, the state $\alpha(t)$ must satisfy the differential equation

$$\dot{\alpha}(t) = -\frac{c_2}{c_3}\alpha(t) + \frac{1}{c_3}e(t).$$

However, this is not true in general, vibrations in the shaft for example cause usually a large $\dot{\alpha}(t)$ and are directly visible in the difference $\omega_\ell(t) - \omega_{\text{ref}}(t)$. So a perfect control performance is not attainable. Even in the steady state ($\dot{\alpha}(t) = 0$) a deviation remains, generated by the state $\alpha(t) \neq 0$, which is proportional to the applied load torque. For this reason, we cannot expect that $\omega_\ell(t)$ converges to a desired setpoint $\omega_{\text{ref}}(\cdot) = \text{const}$.

In Subsection 4.1, (HPF) is introduced with the purpose to cancel the term $c_2\alpha(t)$ in the steady state. The filter generates the additional term $\frac{c_2}{T}\eta(t)$. From (4.7) and $\dot{\eta}(t) = 0$ it follows $\frac{c_2}{T}\eta(t) - c_2\alpha(t) = 0$. Since in the steady state $\dot{\alpha}(t) = 0$ holds true, the deviation $\omega_\ell(t) - \omega_{\text{ref}}(t)$ is proportional to $e(t)$ and can be made arbitrarily small by the funnel controller.

If additionally (PI) is used, then the control error $e(t)$ gets substituted by $-\kappa(t)^{-1} \dot{\xi}(t)$. The benefit is, that a large funnel is applicable (what permits the toleration of measurement noise) without deterioration of the steady state deviation. Since $\dot{\xi} = 0$ if the control loop converges to the steady state, no deviation $\omega_\ell - \omega_{\text{ref}}$ results from e .

The theoretical findings are confirmed by experimental data presented in the following section.

6. EXPERIMENTAL RESULTS

As a practical example, we consider the two mass system depicted in Figure 6.4. This plant is located in the laboratory of the Institute of Electrical Drive Systems, Technical University of Munich, and serves for investigating the behaviour of drives with elastic coupling between motor and mechanics. The four controllers presented in this paper have been tested at it.

In Table I we depict the approximate values of the parameters of the actual two mass system which have been determined by different methods such as calculations based on geometrical data, material constants and physical experiments as well as modern identification strategies, see [1]. Note that the parameters are not used at all for the control. They are given here because they may be informative for a better understanding of the plant used in the experiment.

The actual plant is controlled by the four control schemes (FC), (HPF-FC), (PI-FC) and (HPF-PI-FC) considered in Theorem 5.1 and Corollary 5.2. For all cases, the funnel $\mathcal{F}_\varphi \in \Phi_\lambda$ is defined by the strictly increasing and bounded function

$$t \mapsto \varphi(t) = (150 \cdot \exp\{-2t^2\} + 80)^{-1}.$$

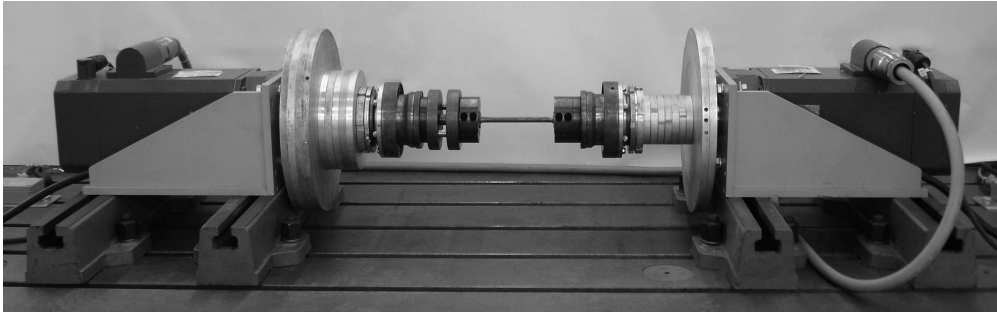


Fig. 6.4. Picture of the two mass system in the laboratory. The dimensions of the elastic shaft are 120 mm (length) and 9 mm (diameter). The overall length of the plant is appr. 1.5 m.

Note that $\lambda = 80$ but $\varphi \notin \Phi_\lambda$ since $\varphi(0) = 1/230$. However, Theorem 5.1 and Corollary 5.2 remain valid as long as $|e(0)| < \varphi(0)^{-1}$. The reference signal $t \mapsto \omega_{\text{ref}}(t) = 30 \cdot (1 - \exp\{-t/0.3\})$ [rad/sec] tends asymptotically to a constant setpoint and is depicted by a dotted line in Fig. 6.5. To examine the rejection of disturbances caused by the driven mechanics, a constant load $M_\ell = 10$ [Nm] is injected at time $t = 10$ [sec]. An input disturbance \hat{d} is not applied externally, but is present due to the non-ideal behaviour of the power converter.

The simulation study in [9] demonstrates the influence of the weighting factor c_2 if funnel control (FC) according to Theorem 5.1 and Corollary 5.2 is used without any extension. It is observed that the friction or a load torque causes a deviation in the steady state; this is typical for proportional controllers. The deviation stays small, if c_2 is small. However, during the transient period large oscillations occur. These oscillations are excited for example if the load changes abruptly or by periodic action of the friction force and cannot be damped by the controller actively as long as the angle of twist is not included in the feedback signal. The damping improves considerably if weighting factor c_2 is enlarged. Then the angle of twist α plays a significant rôle in the feedback signal which yields active damping. However, from Corollary 5.2 (FC) it follows that the deviation $\omega_\ell(t) - \omega_{\text{ref}}(t)$ increases due to the term $c_2 \alpha(t)$, wherein $\alpha(t) = [M_\ell + g\omega_\ell(t) + (\mathbf{N}\omega_\ell)(t)]/k$ depends on the unknown load torque M_ℓ , the unknown parameters g and \mathbf{N} of the friction characteristic and on the unknown stiffness k .

This observation underpins that extensions for funnel control are necessary to obtain desired performance. It seems advantageous, and is confirmed by our experiments, to choose a large value c_2 and to compensate its effects by a PI-controller and a high pass filter. Consequently, a state feedback with a large c_2 is used for the experiments where the design parameter vector c is set to $c = (0.1, 80, 0.5)$.

The different effects of the PI and HPF extensions are depicted in Fig. 6.5 to 6.7. On the left hand side of Fig. 6.5 the speed $\omega_\ell = (1, 0, 0)x$ is depicted together with the desired speed trajectory $\omega_{\text{ref}}(\cdot)$. This figure shows the signals in which the user of the plant is interested in. On the right hand side the output \hat{y} is shown with the appendant reference signal y_{ref} . The output \hat{y} contains all information the controller obtains about the plant.

TABLE I
IDENTIFIED PARAMETERS OF THE TWO MASS SYSTEM.

| | | |
|------------------|-----------|-------------------------------------|
| $J_d = 0.166$ | kgm^2 | moment of inertia (drive mass) |
| $J_\ell = 0.333$ | kgm^2 | moment of inertia (load mass) |
| $d = 0.025$ | Nms/rad | damping coefficient (elastic shaft) |
| $k = 410$ | Nm/rad | stiffness (elastic shaft) |
| $g = 0.0018$ | Nms/rad | viscous friction coefficient |

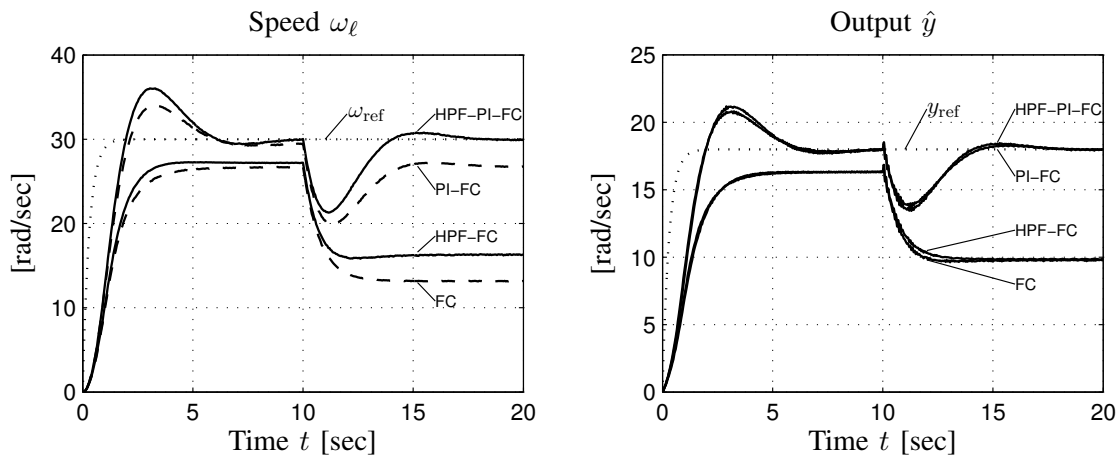


Fig. 6.5. Experimental Results. Left hand side: speed ω_ℓ under funnel control with different extensions; Right hand side: output \hat{y} .

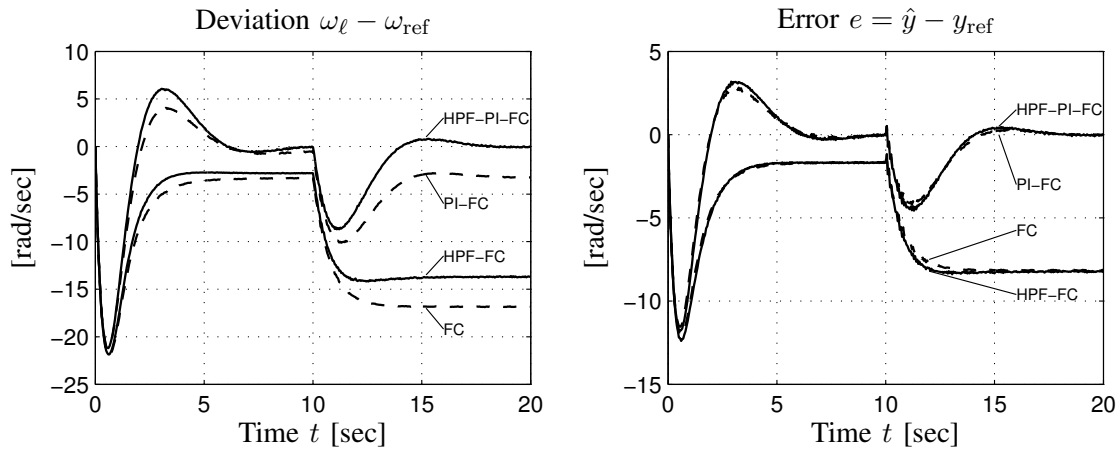


Fig. 6.6. Experimental Results. Left hand side: deviation $\omega_\ell - \omega_{ref}$ under funnel control with different extensions. Right hand side: control error $e = \hat{y} - y_{ref}$.

Due to the choice $c_2 = 80$, all oscillations in the shaft are suppressed adequately. The funnel controller (FC) however is not able to produce steady state accuracy. The friction torque reduces the speed ω_ℓ to approximately 26.7 [rad/sec]. With the additional load (10 [Nm]) the speed slows down to 13.2 [rad/sec], which corresponds to a control error of about 56%.

To improve the accuracy, the PI-controller is employed. The configuration (PI-FC) forces the output \hat{y} to the reference value y_{ref} and reduces the remaining error e to zero asymptotically, even if load is present. Although the controller accomplishes its task ($e \rightarrow 0$), the speed ω_ℓ does not converge to the desired value ω_{ref} . Corollary 5.2 (PI-FC) points out why a deviation remains nevertheless. The angle of twist $\alpha \neq 0$ (caused by friction or load) leads to an additive term and is therefore the reason why the PI-extension is insufficient.

The purpose of the high pass filter is to eliminate the additive term $c_2\alpha$ in (HPF-FC) in Corollary 5.2 without erasing important information from the signal \hat{y} . Further on, oscillations are weighted by $c_2 = 80$ and are included in \hat{y} . Therefore, the desired damping is maintained. In the steady state however the unfavourable effect of a constant $\alpha \neq 0$ is suppressed by the HPF. Because the term $c_2\alpha$ does not longer appear, the deviation is reduced by this value.

The combination of the funnel controller (FC) with $c_2 \neq 0$ together with (HPF) gives, in the steady state, the same value for ω_ℓ as a funnel controller with $c_2 = 0$ does. However, compared to funnel control with $c_2 = 0$ the (HPF-FC) reveals the advantage of better damping.

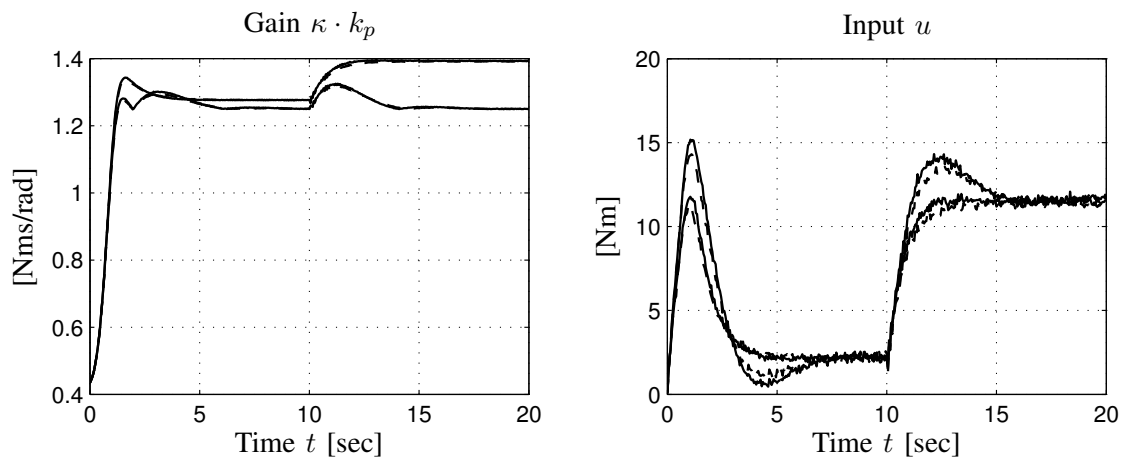


Fig. 6.7. Experimental Results. Left hand side: gain $\kappa \cdot k_p$ under funnel control with different extensions. Right hand side: input u .

These measurement results and theoretical investigations suggest that the extension of funnel control with either (PI) or (HPF) attains not a satisfying improvement. For this reason the overall structure from Fig. 1.2, i.e. (HPF-PI-FC) is tried finally and the results are depicted in Figure 6.5. The integrating contribution in the control action forces $\dot{\xi}$ to vanish, which is equivalent with $e \rightarrow 0$ (see Fig. 6.6). From this, the controlled variable \hat{y} converges to the reference value y_{ref} , even if load is applied. Because (HPF) eliminates the effect of α asymptotically in the feedback signal by cancelling out the term αc_2 , no deviation remains. From this $e \rightarrow 0$ causes ω_ℓ converge to the desired value ω_{ref} .

7. CONCLUSION

We have introduced a control strategy for two mass systems which does not depend on the system data but only on structural system properties. The controller compares in its simplicity favourably to other approaches based on system data identification or neural networks. The model of the two mass system is a functional differential equation which includes nonlinear friction and hysteretic effects. The overall controller preserves the simplicity of the funnel controller but, by invoking a simple high pass filter and a PI-controller, overcomes such drawbacks as nonzero steady state error and no active damping of the shaft oscillation.

REFERENCES

- [1] B.T. Angerer, C. Hintz, and D. Schröder. Online identification of a nonlinear mechatronic system. *Control Engineering Practice*, 12:1465–1478, 2004.
- [2] D. Schröder (Ed.). *Intelligent Observer and Control Design for Nonlinear Systems*. Springer-Verlag, Berlin, 2000.
- [3] W. Hahn. *Stability of Motion*. Springer-Verlag, Berlin, Heidelberg, New York, 1967.
- [4] A. Ilchmann, E.P. Ryan, and C.J. Sangwin. Tracking with prescribed transient behaviour. *ESAIM Control, Opt. and Calculus of Variations*, 7:471–493, 2002.
- [5] A. Ilchmann, E.P. Ryan, and P. Townsend. Tracking with prescribed transient behaviour for nonlinear systems of known relative degree. *SIAM J. of Control and Optim.*, 46:210–230, 2007.
- [6] A. Isidori. *Nonlinear Control Systems*. Springer-Verlag, London, 3 edition, 1995.
- [7] H. Logemann and A.D. Mawby. Low-gain integral control of infinite dimensional regular linear systems subject to input hysteresis. In F. Colonius, U. Helmke, D. Prätzel-Wolters, and F. Wirth, editors, *Advances in Mathematical Systems Theory*, pages 255–293. Birkhäuser Verlag, 2001.
- [8] K. S. Narendra and A. M. Annaswamy. *Stable Adaptive Systems*. Prentice-Hall, London, 1989.
- [9] H. Schuster, C. Westermaier, and D. Schröder. Non-identifier-based adaptive control for a mechatronic system achieving stability and steady state accuracy. In *Proc. 2006 IEEE Int. Conf. on Control Applications, CCA*, pages 1819–1824, Munich, Germany, 2006.